Low-Temperature Growth of Crystalline Gallium Nitride Films Using Vibrational Excitation of Ammonia Molecules in Laser-Assisted Metalorganic Chemical Vapor Deposition

Hossein Rabiee Golgir, Yang Gao, Yun Shen Zhou, Lisha Fan, Premkumar Thirugnanam, Kamran Keramatnejad, Lan Jiang, Jean-François Silvain, Yong Feng Lu

Low-Temperature Growth of Crystalline Gallium Nitride Films Using Vibrational Excitation of Ammonia Molecules in Laser-Assisted Metalorganic Chemical Vapor Deposition

Hossein Rabiee Golgir[†], Yang Gao[†], Yun Shen Zhou[†], Lisha Fan[†], Premkumar Thirugnanam[†], Kamran Keramatnejad[†], Lan Jiang[‡], Jean-François Silvain[§], and Yong Feng Lu[*†]

† *Department of Electrical Engineering, University of Nebraska-Lincoln, Lincoln, Nebraska 68588-0511, United States*
‡ *School of Mechanical Engineering, Beijing Institute of Technology, Beijing 100081, China*
§ *Institut de Chimie de la Matière Condensée de Bordeaux (ICMCB-CNRS) 87, Avenue du Docteur Albert Schweitzer, F-33608 Pessac Cedex, France*

Abstract

Low-temperature growth of crystalline gallium nitride (GaN) films on *c*-plane sapphire (α-Al_2O_3) substrates was achieved by laser-assisted metalorganic chemical vapor deposition (LMOCVD) and coupling laser energy into the chemical reactions. Trimethylgallium (TMGa) and ammonia (NH_3) were used as precursors for the growth of GaN films. Through the resonant excitation of rotational–vibrational transition (1084.71 cm^{-1}) of the NH-wagging mode (v_2) in NH_3 molecules using a wavelength-tunable CO_2 laser tuned at 9.219 μm, highly *c*-axis oriented GaN films were deposited on sapphire at low substrate temperatures from 250 to 600 °C. GaN films with a large thickness of 12 μm were obtained within 1 h at a substrate temperature of 600 °C. The GaN films deposited by LMOCVD showed a higher degree of crystallinity, higher growth rate, and lower defect densities as compared to those synthesized by MOCVD without resonant excitation of NH_3 molecules. This low-temperature synthesis technique opens a promising approach to growing nitrides with low adverse effects.

1 Introduction

Gallium nitride (GaN), a III–V compound semiconductor with a wide, direct band gap of ~3.4 eV, has been utilized in widespread applications, such as optoelectronics and high-power electronic devices. [(1-3)] High-quality crystalline GaN films are in demand for their ability to enhance the performance and reliability of GaN-based devices. [(4-7)] However, growth of high-quality crystalline GaN films requires growth techniques using high temperatures, such as metalorganic chemical vapor deposition (MOCVD, ~950–1100 °C), molecular beam epitaxy (MBE, ~800 °C), and hydride vapor phase epitaxy (HVPE, ~750 °C). [(6-8)] A sufficiently high temperature is necessary to overcome the activation barriers to precursor chemisorption and adatom surface diffusion. However, high substrate temperatures can also cause adverse effects, such as biaxial stress within GaN films, nitrogen loss, and GaN decomposition, which degrade the efficiency of GaN-based devices. [(9-10)] The biaxial stress is caused by the difference between thermal expansion coefficients of the GaN epitaxial layer and substrates (e.g., sapphire and silicon (Si)) and results in a poor light extraction in GaN-based light-emitting diodes (LEDs). [(10)] To reduce the thermal stress in GaN films, substrates with a matching lattice, including lithium aluminate ($LiAlO_2$), lithium gallate ($LiGaO_2$), and silicon carbide (SiC), are preferred. [(11-13)] However, such lattice-matching substrates are too expensive to be commercialized. A high growth temperature will also lead to nitrogen reevaporation and GaN decomposition, which limits the growth rate of GaN films. [(14)] So far, the growth rates of GaN films synthesized by MOCVD and MBE were reported to be 4 and 1 μm/h, respectively. [(15-16)] Therefore, a low-temperature synthetic technique is highly desired in growing crystalline GaN films.

In conventional GaN synthetic methods, energy is added into the gas precursors in the form of thermal heating. Energy is first deposited to kinetic energy of the reactant molecules and eventually makes its way into the internal modes (electronic, vibrational, and rotational) via collisions. [6-8] However, universal thermal heating is short of selectivity in chemical reactions. Attempts at promotion of material synthesis have been investigated by exploring infrared (IR)-laser-assisted vibrational excitations of precursor molecules, in which energy is directly coupled into specific molecules toward selective reaction pathways. [17-18] Highly efficient energy coupling through vibrational excitation provides reactant molecules with sufficient energy to surmount reaction barriers and influence reaction pathways. [19-20] In our previous studies, substantial enhancement in diamond growth was observed with resonant vibrational excitation of ethylene molecules in an IR-laser-assisted combustion CVD process. [21-22]

In this study, low-temperature growth of highly *c*-oriented GaN films was achieved at a growth rate of up to 12 μm/h using laser-assisted metalorganic chemical vapor deposition (LMOCVD). Resonant excitation of the NH-wagging mode (v_2) in NH_3 molecules was realized using a wavelength-tunable carbon dioxide (CO_2) laser at a matching wavelength of 9.219 μm. GaN films were successfully deposited on sapphire at a substrate temperature as low as 250 °C. A GaN growth rate of up to 12 μm/h was achieved at 600 °C using the LMOCVD method, which is 4.6 times faster than that of conventional MOCVD (2.6 μm/h). The influence of laser resonant vibrational excitation of NH_3 on the GaN film growth was investigated.

2 Experimental Section

2.1 Measurement of Laser Power Absorption by NH_3 Molecules

The absorption spectra of CO_2 laser power by gaseous NH_3 were measured in a vacuum chamber with an absorption path length of 40.64 cm (Figure 1). Absorption measurement of laser power at different laser wavelengths (9.2–10.9 μm) was performed at three different gas pressures of 1, 10, and 100 Torr, respectively. In the experiments, the chamber was evacuated to a base pressure of 1×10^{-2} Torr. NH_3 gas was subsequently introduced into the chamber. The incident laser power was kept at 80 W. A power meter was used to measure the laser power before and after passing through the chamber. The drop in laser power was calculated as the absorption percentage.

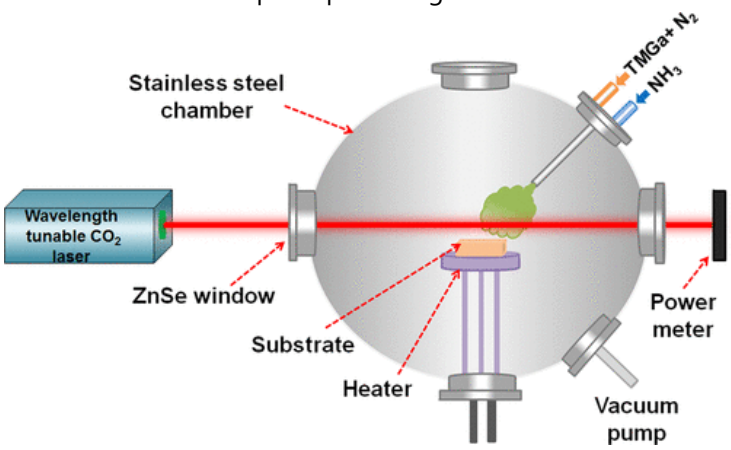

Figure 1. Illustration of the experimental setup for the CO_2 laser-assisted MOCVD growth of GaN films at low temperatures.

2.2 Growth of GaN Films

Figure 1 shows the experimental setup of the LMOCVD system for the growth of crystalline GaN films at low temperatures. GaN films were grown on *c*-plane sapphire substrates at different temperatures (250–600 °C). The sapphire substrates, with a dimension of 10 × 10 mm^2, were ultrasonically cleaned with organic solvents (acetone and methanol) and deionized water, dried, and loaded into the LMOCVD chamber, sequentially. Then, the chamber was evacuated to a base pressure of 1×10^{-2} Torr using a mechanical pump. Trimethylgallium (TMGa) and ammonia (NH_3) precursors were used as gallium (Ga) and nitrogen (N) precursors, respectively. The gas flow rate of NH_3 was 1200 standard cubic centimeters per minute (sccm), and TMGa was carried into the reaction chamber using nitrogen as the carrying gas at a flow rate of 16 sccm. The growth pressure was maintained at 100 Torr during the growth process. A wavelength-tunable CO_2 laser (PRC, wavelength range

from 9.2 to 10.9 μm) was used to achieve resonant vibrational excitation of the NH_3 molecules. The laser was tuned at a wavelength of 9.219 μm with a power of 80 W to resonantly excite the rotational–vibrational transition of the NH-wagging mode (ν_2, 1084.63 cm^{-1}) of NH_3 molecules and couple the laser energy into the molecules. The laser beam, with a diameter of around 6–9 mm, was irradiated in parallel to the substrate surface inside the chamber through a zinc selenide (ZnSe) window, as shown in Figure 1. The distance between the laser beam and substrate surface was maintained at about 20 mm. The substrate temperature was maintained at a constant temperature of 150, 250, 350, 450, and 600 °C, respectively. The deposition time was kept at 1 h. To understand the effects of laser-induced energy coupling, GaN films were also synthesized by the conventional MOCVD technique under the same growth conditions (deposition temperature, deposition time, gas flow rate, and growth pressure) without laser irradiation.

2.3 Characterization of GaN Films

The crystallinity of the GaN films was examined using a powder X-ray diffractometer (Rigaku D/Max B diffractometer, Co $K\alpha_1$ λ = 1.788 Å). Surface morphologies and dimensions of the GaN films were studied using a field emission scanning electron microscope (FESEM, S4700). An energy-dispersive X-ray spectrometer (EDX, Oxford X-max 20 mm^2) was applied to analyze the composition of the GaN films. The optical properties of GaN films were studied using a photoluminescence spectrometer (iHR320 photoluminescence spectrometer with Si detector and indium gallium arsenide (InGaAs) detector).

3 Results and Discussion

3.1 Roles of Resonant Vibrational Excitation of NH_3 in GaN Growth

NH_3 is a dominant nitrogen source in GaN synthesis. However, NH_3 has low decomposition efficiency due to a high NH bond energy (93–105 kcal/mol). [23] A sufficient amount of active N species are required for GaN growth. The growth rate of GaN depends on the molecular flux of active N and Ga species that transport to substrates. [24] However, it is difficult to grow GaN films at temperatures lower than 500 °C using a conventional MOCVD method due to the low dissociation efficiency of NH_3. [23] To increase the reactivity of NH_3 is, therefore, critical in low-temperature growth of GaN. Through resonant vibrational excitation of the NH-wagging mode in NH_3 molecules, the reactivity of NH_3 is selectively enhanced, and the dissociation efficiency of NH_3 at low temperature is promoted. [25-26]

The absorption spectra of the CO_2 laser power by NH_3 gas at different gas pressures of 1, 10, and 100 Torr are shown in Figure 2. Three strong absorption peaks were observed at 9.219, 10.35, and 10.719 μm, respectively, at the NH_3 pressures of 10 and 100 Torr. At a pressure of 100 Torr, the laser energy at these three wavelengths was completely absorbed by NH_3 gas, whereas only one absorption peak at 9.219 μm was observed at a pressure of 1 Torr. The absorptions at these wavelengths were attributed to the resonant vibrational excitation of the NH-wagging mode (ν_2) of the NH_3 molecules. [25-26] NH_3 has a pyramidal shape with three hydrogen atoms forming the base and a nitrogen atom at the top. The NH-wagging mode vibrates in an umbrella inversion way. There is a barrier to umbrella inversion that the nitrogen atom faces on its travels through the hydrogen plane. [25] The existence of the barrier results in a splitting of a fundamental vibrational level of the NH-wagging mode into two components at 932.51 (ν_2+) and 968.32 (ν_2−) cm^{-1}, giving rise to the observed absorption peaks at laser wavelengths of 10.719 (932.92 cm^{-1}) and 10.35 μm (966.18 cm^{-1}), respectively. [25-26] The strongest absorption peak at 9.219 μm is attributed to a rotational–vibrational transition (J = 5 → J′ = 6, K = 0) of the ν_2 mode at 1084.63 cm^{-1}. The perfect match between the CO_2 laser wavelength at 9.219 μm (1084.71 cm^{-1}) and the rotational–vibrational transition line of the NH_3 (1084.63 cm^{-1}) makes a stronger absorption at 9.219 μm than that at 10.35 and 10.719 μm. The rotational–vibrational excitation of NH_3 molecules at 9.219 μm contributes to dissociating of NH_3 molecules at low temperatures.

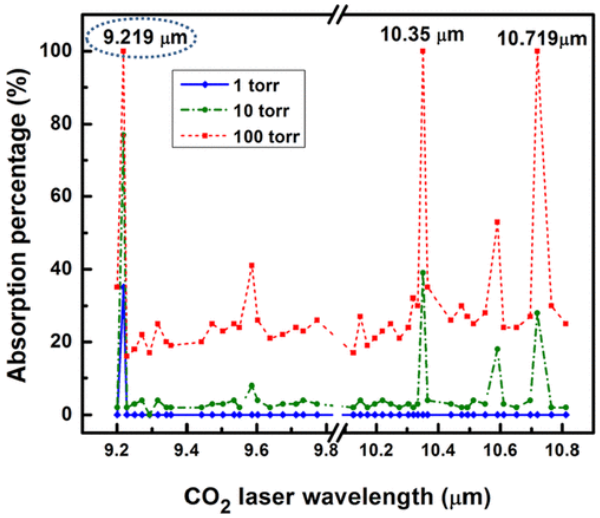

Figure 2. Absorption of CO_2 laser energy by NH_3 from 9.219 to 10.8 μm at pressures of 1, 10, and 100 Torr.

3.2 Characterization of GaN Films

The X-ray diffraction (XRD) 2θ spectra of the GaN films grown at different temperatures (i.e., 150, 250, 350, 450, and 600 °C) are shown in Figure 3. Panels (a) and (b) in Figure 3 compare the XRD 2θ patterns of the GaN films grown by LMOCVD and MOCVD, respectively. A XRD peak attributed to the (0002) plane of GaN is observed in the GaN samples grown by LMOCVD at temperatures from 250 to 600 °C. This peak is indexed to wurtzite GaN with a hexagonal structure, [27] indicating the high *c*-plane orientation of the GaN films. Therefore, it can be confirmed that the synthesis of GaN films was achieved at a temperature as low as ~250 °C by the LMOCVD technique with the laser resonant vibrational excitation of NH_3. In contrast, the (0002) diffraction peak was only found for the sample grown by MOCVD at a temperature of 600 °C, suggesting that a much higher substrate temperature is required for the growth of GaN using conventional MOCVD (Figure 3b). As shown in Figure 3a, the intensity of the (0002) peak increases as the substrate temperature increases from 250 to 600 °C. The intensity increase can be attributed to the improved crystalline quality of the GaN films due to the substrate temperature increase. [28] Additionally, a 2θ signal at 86° was observed for the GaN film grown at 600 °C with LMOCVD (Figure 3a). This (0004) GaN peak also refers to *c*-axis oriented GaN films.

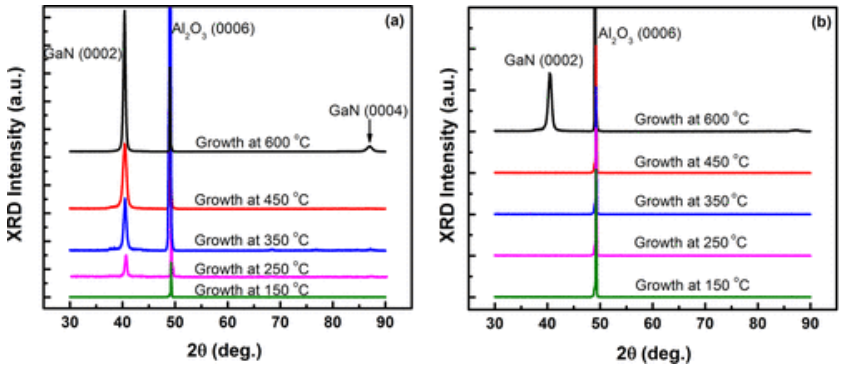

Figure 3. X-ray diffraction spectra of the GaN films grown on sapphire substrates at different temperatures (250–600 °C) by (a) LMOCVD and (b) MOCVD.

The XRD φ-scan determined the degree of in-plane alignment of GaN films grown at different temperatures (250–600 °C) by LMOCVD relative to the sapphire substrate, as shown in Figure 4. The scanning planes used for φ-scan were $(11\bar{2}0)$ for sapphire and hexagonal $(10\bar{1}1)$ and cubic (200) for GaN films. The diffraction peaks from the $(10\bar{1}1)$ plane of the GaN film were observed at intervals of 60° for all samples grown at temperatures from 250 to 600 °C, which confirmed the hexagonal structure of the epitaxial GaN films. It is also observed that there is a ~30° rotation of the GaN unit cell with respect to the sapphire substrate due to the large lattice mismatch between GaN and the sapphire substrate (Figure 4). However, no diffraction peaks from the (200) plane of cubic GaN film were observed for all samples grown at different temperatures (250–600 °C) by LMOCVD (see the Supporting Information, Figure S1).

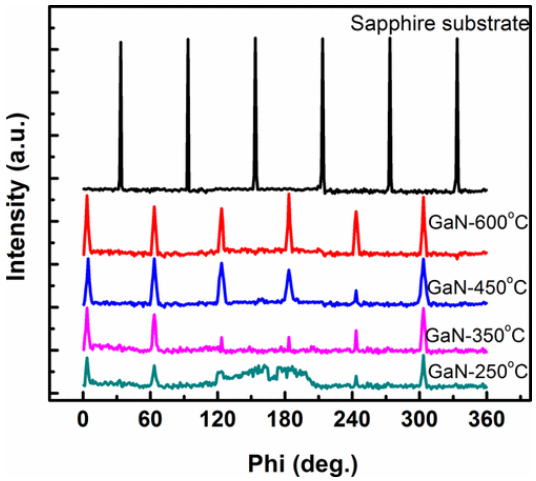

Figure 4. XRD φ-scan of (11$\bar{2}$0) plane of the sapphire substrate and (10$\bar{1}$1) plane of GaN films grown on sapphire at different temperatures (250–600 °C) by LMOCVD.

The 2θ position and full width at half-maximum (FWHM) of (0002) diffraction peaks obtained from XRD are shown in Table 1. The FWHM of the (0002) plane reflects lattice distortion from screw dislocations and mixed dislocations. [28] As shown in Table 1, a small FWHM value of 0.18° was obtained for the GaN sample grown by LMOCVD at 600 °C. For the GaN film grown by MOCVD at 600 °C, the FWHM of (0002) was 0.20°. The distinctive reduction in the FWHM of GaN films deposited by LMOCVD indicates that the laser resonant vibrational excitation of NH_3 leads to a decrease in lattice distortion and improvement in the quality of the GaN films. For the GaN films grown by LMOCVD, the FWHM of the (0002) plane decreased monotonically with the increase in the substrate temperature from 250 to 600 °C (Table 1). This means that the crystalline quality of GaN films improves continuously with the increase in the growth temperature, which is explained by the reduction in diffusion barriers and the increase in diffusion rates of Ga and N species as the substrate temperature increases. [28]

Table 1. GaN (0002) Diffraction Peak Position, FWHM of (0002) Plane, Growth Rate of GaN Films, and the Grain Size of GaN Films Grown at Different Temperatures (250−600 °C)

sample	substrate temperature (°C)	2θ (deg)	FWHM of (0002) (deg)	growth rate (μm/h)	grain size (nm)
LMOCVD	250	40.55	0.27	0.15	30 ± 5
LMOCVD	350	40.60	0.25	0.60	65 ± 10
LMOCVD	450	40.42	0.21	1.60	100 ± 10
LMOCVD	600	40.40	0.18	12	200 ± 10
MOCVD	600	40.47	0.20	2.60	120 ± 10

The effectiveness of laser resonant vibrational excitation of NH_3 on the uniformity and surface morphology of GaN films is clearly shown by the FESEM images shown in Figure 5. For the GaN film grown with LMOCVD at 250 °C (Figure 5a), small domains of about ~30 ± 5 nm with hexagonal facets were obtained. The average domain sizes were ~65 ± 10 and ~100 ± 10 nm for the GaN films grown by LMOCVD at 350 and 450 °C, respectively (Figure 5b,c). With a further increase in the substrate temperature to 600 °C, the lateral size of the islands with hexagonal facets increased. With a coalescence of crystallite islands, GaN structures with flat facets were obtained by LMOCVD at 600 °C, as shown in Figure 5d. In contrast, the surface of the GaN sample grown at 600 °C by MOCVD was rough with obvious hexagonal hillocks (Figure 5f). Additionally, the threshold temperature to grow GaN films by MOCVD is 600 °C. Below this temperature, no GaN deposition is observed on the substrate surfaces (Figure 5e), which agrees with the XRD results.

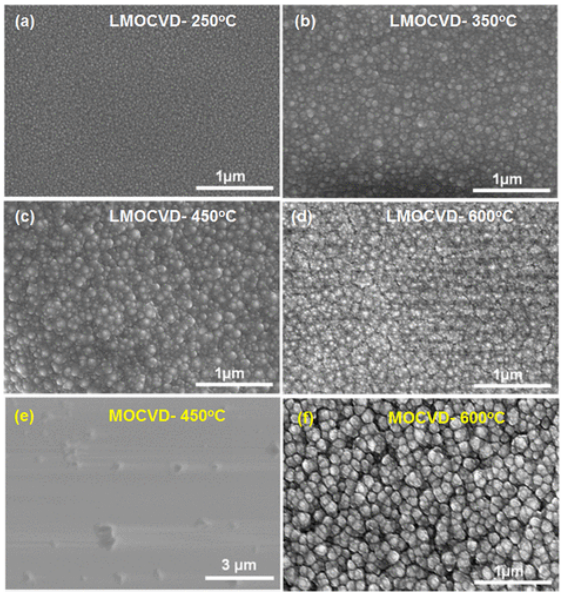

Figure 5. SEM images of GaN films grown by LMOCVD at temperatures of (a) 250, (b) 350, (c) 450, and (d) 600 °C; and SEM images of GaN films grown by MOCVD at temperatures of (e) 450 and (f) 600 °C.

The cross-sectional SEM images of the GaN films were obtained to explore the effect of laser resonant vibrational excitation of NH_3 on the growth rate. Figure 6a,b shows the cross-sectional SEM images of the GaN films grown at 600 °C by LMOCVD and MOCVD, respectively. A growth rate of 12 μm/h was achieved by LMOCVD, which is ~4.6 times faster than that of MOCVD (this work, ~2.6 μm/h). Moreover, compared with the growth rate of GaN synthesized by other studies (MBE: ~1 μm/h; and MOCVD: ~4 μm/h), [15-16] laser resonant vibrational excitation contributes to a drastic enhancement in the GaN growth rate. Table 1 shows the GaN growth rates by LMOCVD at different temperatures from 250 to 600 °C. As the substrate temperature increased, the thickness of the GaN films increased.

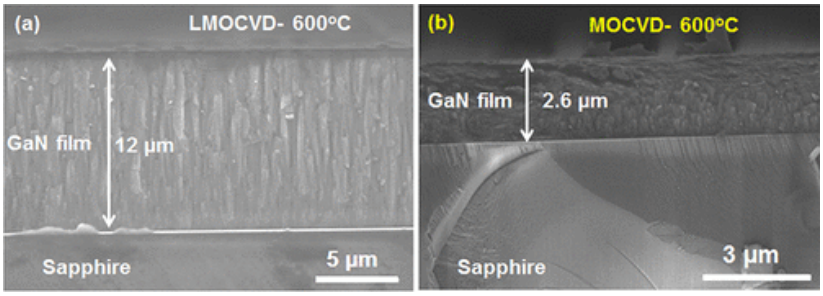

Figure 6. Cross-sectional SEM images of GaN films grown at 600 °C by (a) LMOCVD and (b) MOCVD.

The EDX results in Figure 7 confirm the presence of Ga and N elements in the GaN films, as well as carbon (C), oxygen (O), and silicon (Si) as impurities. According to the EDX spectra obtained from GaN films grown at 600 °C by LMOCVD and MOCVD, obvious increases of 7.84% in N concentration and 1.7% in Ga concentration were observed in the sample grown with LMOCVD. The resonant vibrational excitation of the NH bond vibration in NH_3 molecules plays an important role in the dissociation of NH_3 and the increase of N species in the reaction. The increase in N content in the deposited films explains why the GaN growth rate was highly improved using LMOCVD, which is in agreement with other studies. [29] Furthermore, it is worthy to note that the impurity content (C, O, and Si) in the GaN film grown with LMOCVD decreased considerably (Figure 7). In MOCVD growth, Ga reacts with impurity elements in the absence of sufficient active N atoms or N-related intermediates. However, laser resonant vibrational excitation of NH_3 in LMOCVD increased the production of active N-related intermediates, eliminating the impurity content incorporated into the film during GaN growth. With the reduction in impurities, the GaN crystal islands grow larger in size, leading to higher crystallinity, a full coalescence, and a smooth surface morphology of GaN films (Figure 5d). It is also worthy to note that EDX measurements here just express a semiquantitative analysis and the values do not reflect the actual composition of the GaN films. [30] The large concentration of oxygen and carbon in the films is just an artifact resulting from the very low detection efficiency of EDX for light elements.

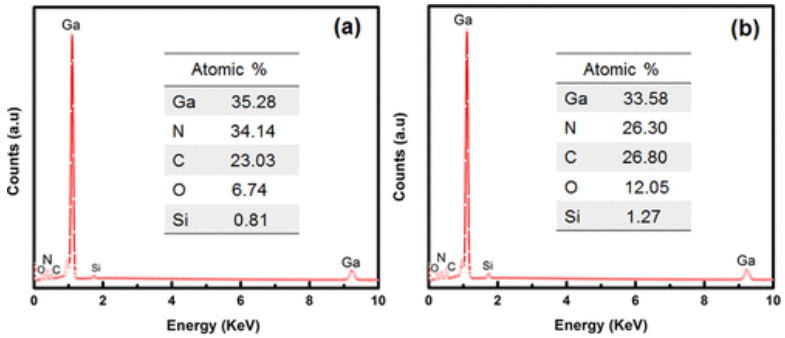

Figure 7. EDX spectra of GaN films grown at 600 °C by (a) LMOCVD and (b) MOCVD.

The optical quality of the GaN films was studied using a photoluminescence spectrometer at room temperature (see the Supporting Information, Figure S2). The GaN film grown at 600 °C by LMOCVD showed a near-band-edge (NBE) emission at about ~3.398 eV, which was closer to the NBE emission of bulk GaN (3.47 eV), [31] compared to that of MOCVD with ~3.394 eV. The NBE peaks of GaN films grown by LMOCVD at 250, 350, and 450 °C are ~3.388, ~3.391, and ~3.392 eV, respectively.

It is valuable to note that there are several studies of using the polycrystalline GaN films with columnar structures for photonic and electronic devices. [32-33] In this study, the quality of the polycrystalline GaN films grown at low temperatures by LMOCVD are comparable to those reported values, [32-33] suggesting a potential of polycrystalline GaN film grown by LMOCVD for electronic and photonic applications.

4 Conclusions

The LMOCVD technique was developed for low-temperature growth of GaN films on sapphire substrates through laser resonant vibrational excitation of NH_3 molecules. The highly *c*-oriented GaN films were successfully grown at temperatures as low as 250 °C. Low-temperature growth of GaN films is ascribed to the enhanced decomposition efficiency of NH_3 with resonant excitation of rotational–vibrational transition (1084.71 cm^{-1}) of the NH-wagging mode at the laser wavelength of 9.219 μm. The FWHM of (0002) diffraction peaks obtained from XRD for GaN films grown at 600 °C decreased from 0.20° (MOCVD) to 0.18° (LMOCVD), indicating an improvement in crystalline quality by LMOCVD. SEM images showed that the laser resonant vibrational excitation of NH_3 helped to grow GaN films with a smooth and uniform surface morphology. A high GaN growth rate of up to 12 μm/h was achieved at 600 °C by LMOCVD, which is ~4.6 times faster than that of conventional MOCVD with 2.6 μm/h. This approach suggests that the laser resonant vibrational excitation of precursors is promising in increasing NH_3 reactivity and promoting GaN synthesis, which could be extended to the synthesis of other nitride semiconductors.

Supporting Information

XRD ϕ-scan of (200) plane of GaN films grown by LMOCVD and PL spectra of GaN films acquired with a 325 nm laser. This material is available free of charge via the Internet at http://pubs.acs.org.

Author Information

- *Corresponding Author :*
  Yong Feng Lu - Department of Electrical Engineering, University of Nebraska-Lincoln, Lincoln, Nebraska 68588-0511, United States; Email: ylu2@unl.edu
- *Authors :*
  Hossein Rabiee Golgir - Department of Electrical Engineering, University of Nebraska-Lincoln, Lincoln, Nebraska 68588-0511, United States
  Yang Gao - Department of Electrical Engineering, University of Nebraska-Lincoln, Lincoln, Nebraska 68588-0511, United States

Yun Shen Zhou - Department of Electrical Engineering, University of Nebraska-Lincoln, Lincoln, Nebraska 68588-0511, United States
Lisha Fan - Department of Electrical Engineering, University of Nebraska-Lincoln, Lincoln, Nebraska 68588-0511, United States
Premkumar Thirugnanam - Department of Electrical Engineering, University of Nebraska-Lincoln, Lincoln, Nebraska 68588-0511, United States
Kamran Keramatnejad - Department of Electrical Engineering, University of Nebraska-Lincoln, Lincoln, Nebraska 68588-0511, United States
Lan Jiang - School of Mechanical Engineering, Beijing Institute of Technology, Beijing 100081, China
Jean-François Silvain - Institut de Chimie de la Matière Condensée de Bordeaux (ICMCB-CNRS) 87, Avenue du Docteur Albert Schweitzer, F-33608 Pessac Cedex, France

- *Notes :*
  The authors declare no competing financial interest.

Acknowledgment

This work was financially supported by the National Science Foundation (NSF CMMI 1068510 and 1129613). It was also performed in part in the Central Facilities of the Nebraska Center for Materials and Nanoscience, which is supported by the Nebraska Research Initiative.

References

1. Khan, A.; Balakrishnan, K.; Katona, T. Nat. Photonics **2008**, 2, 77– 84
2. Avramescu, A.; Lermer, T.; Müller, J.; Eichler, C.; Bruederl, G.; Sabathil, M.; Lutgen, S.; Strauss, U. Appl. Phys. Express **2010**, 3, 061003
3. Wu, Y.-F.; Kapolnek, D.; Ibbetson, J. P.; Parikh, P.; Keller, B. P.; Mishra, U. K. IEEE Trans. Electron Devices **2001**, 48, 586– 590
4. Cheng, K.; Leys, M.; Degroote, S.; Germain, M.; Borghs, G. Appl. Phys. Lett. **2008**, 92, 192111
5. Hashimoto, T.; Wu, F.; Speck, J. S.; Nakamura, S. Nat. Mater. **2007**, 6, 568– 571
6. Gogova, D.; Kasic, A.; Larsson, H.; Hemmingsson, C.; Monemar, B.; Tuomisto, F.; Saarinen, K.; Dobos, L.; Pécz, B.; Gibart, P.; Beaumont, B. J. Appl. Phys. **2004**, 96, 799– 806
7. Gibart, P. Rep. Prog. Phys. **2004**, 67, 667
8. Vézian, S.; Natali, F.; Semond, F.; Massies, J. Phys. Rev. B **2004**, 69, 125329
9. Waltereit, P.; Brandt, O.; Trampert, A.; Grahn, H.; Menniger, J.; Ramsteiner, M.; Reiche, M.; Ploog, K. Nature **2000**, 406, 865– 868
10. Nakamura, S. Science **1998**, 281, 956– 961
11. Ke, X.; Jun, X.; Peizhen, D.; Yongzong, Z.; Guoqing, Z.; Rongsheng, Q.; Zujie, F. J. Cryst. Growth **1998**, 193, 127– 132
12. Sakurada, K.; Kobayashi, A.; Kawaguchi, Y.; Ohta, J.; Fujioka, H. Appl. Phys. Lett. **2007**, 90, 211913
13. Kim, M.; Oshima, M.; Kinoshita, H.; Shirakura, Y.; Miyamura, K.; Ohta, J.; Kobayashi, A.; Fujioka, H. Appl. Phys. Lett. **2006**, 89, 031916
14. Koleske, D.; Wickenden, A.; Henry, R.; Culbertson, J.; Twigg, M. J. Cryst. Growth **2001**, 223, 466– 483
15. Yang, Z.; Li, L.; Wang, W. Appl. Phys. Lett. **1995**, 67, 1686– 1688
16. Nakamura, S.; Harada, Y.; Seno, M. Appl. Phys. Lett. **1991**, 58, 2021– 2023
17. Zare, R. N. Science **1998**, 279, 1875– 1879
18. Crim, F. F. Science **2007**, 316, 1707
19. Killelea, D. R.; Campbell, V. L.; Shuman, N. S.; Utz, A. L. Science **2008**, 319, 790– 793
20. Gao, Y.; Zhou, Y.; Park, J.; Wang, H.; He, X.; Luo, H.; Jiang, L.; Lu, Y. Nanotechnology **2011**, 22, 165604
21. Xie, Z.; Zhou, Y.; He, X.; Gao, Y.; Park, J.; Ling, H.; Jiang, L.; Lu, Y. Cryst. Growth Des. **2010**, 10, 1762– 1766
22. Xie, Z. Q.; He, X. N.; Hu, W.; Guillemet, T.; Park, J. B.; Zhou, Y. S.; Bai, J.; Gao, Y.; Zeng, X. C.; Jiang, L.; Lu, Y. Cryst. Growth Des. **2010**, 10, 4928– 4933
23. Shen, B.; Zhou, Y.; Chen, Z.; Chen, P.; Zhang, R.; Shi, Y.; Zheng, Y.; Tong, W.; Park, W. Appl. Phys. A: Mater. Sci. Process. **1999**, 68, 593– 596
24. Mesrine, M.; Grandjean, N.; Massies, J. Appl. Phys. Lett. **1998**, 72, 350– 352
25. David, C. W. J. Chem. Educ. **1996**, 73, 46

26. Fan, L.; Xie, Z.; Park, J.; He, X.; Zhou, Y.; Jiang, L.; Lu, Y. J. Laser Appl. **2012**, 24, 022001
27. Brandt, O.; Waltereit, P.; Ploog, K. H. J. Phys. D: Appl. Phys. **2002**, 35, 577
28. Kushvaha, S.; Kumar, M. S.; Maurya, K.; Dalai, M.; Sharma, N. D. AIP Adv. **2013**, 3, 092109
29. Iliopoulos, E.; Adikimenakis, A.; Dimakis, E.; Tsagaraki, K.; Konstantinidis, G.; Georgakilas, A. J. Cryst. Growth **2005**, 278, 426– 430
30. Biju, K. P.; Subrahmanyam, A.; Jain, M. K. J. Cryst. Growth **2009**, 311, 2275– 2280
31. Chin, A. H.; Ahn, T. S.; Li, H.; Vaddiraju, S.; Bardeen, C. J.; Ning, C. Z.; Sunkara, M. K. Nano Lett. **2007**, 7, 626– 631
32. Yagi, S. Appl. Phys. Lett. **2000**, 76, 345– 347
33. Bour, D. P.; Nickel, N. M.; Van de Walle, C. G.; Kneissl, M. S.; Krusor, B. S.; Mei, P.; Johnson, N. M. Appl. Phys. Lett. **2000**, 76, 2182– 2184